LUND UNIVERSITY

Fracture Mechanics of Layered Materials

Ståhle, P.

Published in:
Mechanical Behaviour of PVD Coated Materials

1997

Document Version:
Publisher's PDF, also known as Version of record

Link to publication

Citation for published version (APA):
Ståhle, P. (1997). Fracture Mechanics of Layered Materials. In H. Oettel, S. Hogmark, & J. V. Stebut (Eds.), *Mechanical Behaviour of PVD Coated Materials: proceedings of the International Workshop, October 13 - 17, 1997 in Holzhau* (pp. 131-148). TU Bergakademie.

Total number of authors:
1

Creative Commons License:
Unspecified

General rights
Unless other specific re-use rights are stated the following general rights apply:
Copyright and moral rights for the publications made accessible in the public portal are retained by the authors and/or other copyright owners and it is a condition of accessing publications that users recognise and abide by the legal requirements associated with these rights.
• Users may download and print one copy of any publication from the public portal for the purpose of private study or research.
• You may not further distribute the material or use it for any profit-making activity or commercial gain
• You may freely distribute the URL identifying the publication in the public portal

Read more about Creative commons licenses: https://creativecommons.org/licenses/

Take down policy
If you believe that this document breaches copyright please contact us providing details, and we will remove access to the work immediately and investigate your claim.

LUND UNIVERSITY

PO Box 117
221 00 Lund
+46 46-222 00 00

Fracture Mechanics of Coated Materials

P. Ståhle
Luleå University of Technology, division of Solid Mechanics
SE-971 87 Luleå, Sweden; Phone: +46 (0)920 72188,
Fax: +46 (0)920 91047, E-mail: pers@mt.luth.se

1 Basic Equations in Continuum Mechanics

Field equations govern the behavior of solids. In this section the necessary equations are given for Cartesian coordinates, x_i. In the following indices i, j, k... assume the values 1, 2 and 3. The summation convention is used whenever two equal indices appear in a term.

Boundary tractions T_i are related to the stress tensor σ_{ij} via Cauchy's formula

$$T_i = \nu_j \sigma_{ij} \ . \qquad (1)$$

where ν_j is the outward normal to the surface of the body (see Fig. 1). Here only static cases are considered. Thus, equilibrium is required,

$$\sigma_{ij,j} = 0 \ . \qquad (2)$$

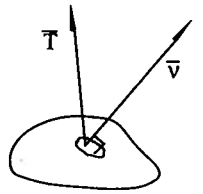

Fig. 1 Traction T and outward normal ν

The strain tensor ε_{ij} with six components is derived from three displacement components, u_i. Because of this, all six components cannot be independent. To ensure the dependence between the strain components either equations of compatibility may be used or, as here, a definition of strain based on displacements is used. Strain is assumed to be small and is defined as follows

$$\varepsilon_{ij} = \tfrac{1}{2}(u_{i,j} + u_{j,i}) \quad . \tag{3}$$

Finally a constitutive relation between stress and strain is needed,

$$\sigma_{ij} = C_{ijkl}\,\varepsilon_{kl} \quad , \tag{4}$$

where C_{ijkl} may be a function of strain, time derivatives of strain, temperature, etc. For isotropic linear elastic materials C_{ijkl} only contain two independent material parameters. One selection is Lamés' constants G (shear modulus) and λ,

$$C_{ijkl} = 2G\delta_{ik}\delta_{jl} + \lambda\delta_{ij}\delta_{kl} \tag{5}$$

where

$$G = \frac{E}{2(1+\nu)} \qquad \text{and} \qquad \lambda = \frac{E\nu}{(1+\nu)(1-2\nu)} \quad . \tag{6}$$

Here E is Young's modulus and ν is Poisson's ratio.

2 Boundary Conditions Near Crack-tips

It is convenient to separate general solutions into symmetric antisymmetric and antiplane parts. Plane symmetric deformation, so called mode I is characterized by

$$\begin{aligned} u_1(x_1, x_2) &= u_1(x_1, -x_2), \\ u_2(x_1, x_2) &= -u_2(x_1, -x_2) \end{aligned} \tag{7}$$

(see Fig. 2a). Plane antisymmetric deformation, mode II, is characterized by

$$\begin{aligned} u_1(x_1, x_2) &= -u_1(x_1, -x_2), \\ u_2(x_1, x_2) &= u_2(x_1, -x_2) \end{aligned} \tag{8}$$

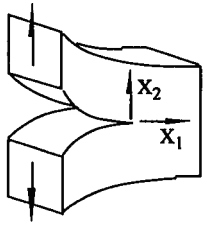

Fig. 2a Mode I

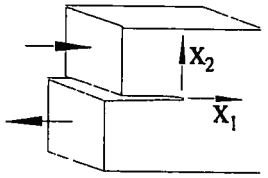

Fig. 2b Mode II

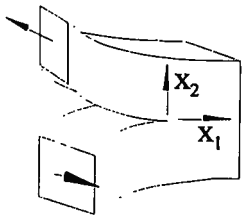

Fig. 2c Mode III

shown in Fig. 2b. Finally antiplane deformation, mode III is an out-of-plane displacement case, characterized by

$$\begin{aligned} u_1 &= u_2 = 0, \\ u_3(x_1, x_2) &= -u_3(x_1, -x_2) \end{aligned} \tag{9}$$

(see Fig. 2c). The plane cases are either plane stress or plane strain cases.

An analytical solution for the stress and strain field at a crack-tip in a linear elastic body was given by the Kolosov (1909) and Inglis (1913). The near-tip solution for stresses and displacements is as follows:

$$\sigma_{ij} = \frac{K_I}{\sqrt{2\pi r}} f_{ij}^{I}(\theta) + \frac{K_{II}}{\sqrt{2\pi r}} f_{ij}^{II}(\theta) + \frac{K_{III}}{\sqrt{2\pi r}} f_{ij}^{III}(\theta) \quad , \tag{10}$$

$$\begin{aligned} u_i = {} & \frac{(1+\nu)K_I}{4\pi E}\sqrt{2\pi r}\, g_i^{I}(\theta) + \frac{(1+\nu)K_{II}}{4\pi E}\sqrt{2\pi r}\, g_i^{II}(\theta) \\ & + \frac{(1+\nu)K_{III}}{4\pi E}\sqrt{2\pi r}\, g_i^{III}(\theta) \end{aligned} \quad , \tag{11}$$

where $r = (x_1^2 + x_2^2)^{1/2}$, $\theta = \tan^{-1}(x_2/x_1)$, K_I, K_{II} and K_{III} are the stress intensity factors and f_{ij} and g_i are known functions of θ. The solution represents the dominating term in a series expansion around the crack-tip, cf. Williams [1]. The complete solution, e.g., for mode I may be given as,

$$\sigma_{ij} = \frac{K_I}{\sqrt{2\pi r}} f_{ij}(\theta) + \sum_{k=\pm1,\pm2,..} \alpha_{ij}^{(k)}\, r^{\frac{1+k}{2}} \quad . \tag{12}$$

where $\alpha_{ij}^{(k)}$ are known angular functions.

3. Autonomy and Crack-tip Modeling

Suitable scaling is obtained by introducing R as a geometry parameter such as ligament width, crack length, etc., and the parameter r_p which represents the size of a non-linear region at the crack-tip. This allow us to do the following separation of (12)

$$\sigma_{ij}/\sigma_o = \left(2\pi r/r_p\right)^{-1/2} f'_{ij}(\theta) + \sum_{k=1,2,..} \alpha'_k \,(r/R)^{\frac{k-1}{2}} + \sum_{k=1,2,..} \alpha'_{-k}\,(r/r_p)^{\frac{-1+k}{2}}, \quad (13)$$

where σ_o is the yield stress. The extent of the non-linear region r_p scale with $(K_I/\sigma_o)^2$.

At small scale yielding there is a circular region A (see Fig. 3) around the crack-tip in which the stress field closely coincides with the field given by the singular stress terms (r^{-1}, $r^{-3/2}$, etc.) in (13). In an annular region B ($r \geq R_B$) only the square-root singular stress term and non-singular terms are significant. Thus, the non-linear near-tip field can be determined by studying a circular disc with the radius R_B using boundary conditions given by K_I. The conclusion is that K_I completely describes the solution in region A and, thus, also the state of the fracture process region at the crack-tip.

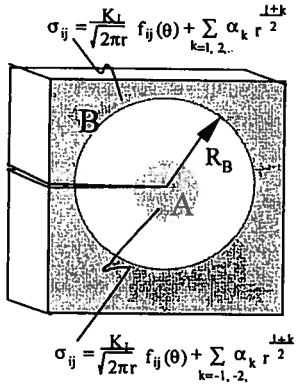

Fig. 3 The state inside A is controlled by K_I.

The square-root singular term together with the non-singular stress terms ($r^{-1/2}$, $r^{1/2}$, etc.) are depending on boundary conditions but the only term communicating information to the non-linear region is the square-root singular term defined by K_I. The non-singular terms of (13) given on the boundary of the body only contribute to the stress state outside region A. According to the principle of superposition all non singular terms may be removed or changed without effecting the state of the non-linear region A including the fracture process region. The non-linear region is said to be autonomous and governed by a single parameter, e.g., K_I, [2, 3]. At linear fracture mechanics the state of the fracture process region, in the sense of growth, growth rate, closure, etc. is controlled by K_I. Fracture mechanical testing is used to correlate K_I with the different states of the process region, e.g., initiation of crack growth, K_{Ic}, threshold for fatigue crack growth, K_{th}, etc.

In cases where R_B extends to the remote boundary or A cease to exist autonomy may be based K_I and one or more second order terms α_{+1}, α_{+2},.. or on parameters derived for elastic plastic solutions, e.g., J or J and Q or other yet unknown parameters.

A theory may also be based on studies of micromechanical studies of fracture processes.

4 Engineering Linear Fracture Mechanics

The practical application of linear elastic fracture mechanics (LEFM) is the transfer of results between tests and applications. The foundation is the K_I governed autonomy of the non-linear region. The limits for LEFM were established by Brown and Shrawley in an ASTM convention [4]. They formulated the following requirements

$$t, a, b > 2.5\left(\frac{K_{Ic}}{\sigma_o}\right)^2 , \quad (14)$$

where t, a and b are thickness crack length and ligament width respectively, K_{Ic} is the fracture toughness.

Assume that a structure is subjected to a load P, e.g., as defined in Fig. 4. With a given geometry the stress intensity factor, K_I, may be determined as a function of P,

$$K_I = K_I(P) \quad . \quad (15)$$

Fracture mechanical testing on a small test specimen (see Fig. 5a), suitable for a laboratory experiment, provide, e.g., crack length, a, as a function of K_I,

$$a = a(K_I) \quad , \quad (16)$$

as suggested in Fig. 5b. By combining (15) and (16) one obtains

$$a = a(P) \quad . \qquad (17)$$

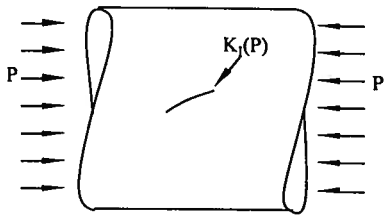

Fig. 4. A crack in engineering structure will be judged on the basis of a lab test

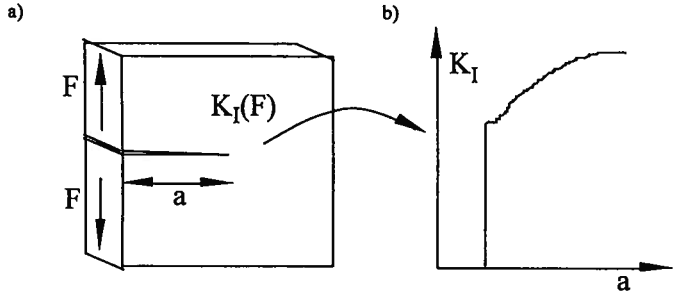

Fig. 5. Fracture mechanical testing may be performed on a small test specimen; a) test specimen and b) test result

5 J - A Path Independent Integral

Consider a linear elastic body in equilibrium (2). Let us use Gauss' theorem on the area integral defined for a regular region with the boundary Γ.

$$I_k = \int \sigma_{ij,j} u_{i,k} dV = -\int \sigma_{ij} u_{i,jk} dV + \int (\sigma_{ij} u_{i,k})_{,j} dV = -\int \sigma_{ij} \varepsilon_{ij,k} dV + \int (\sigma_{ij} u_{i,k})_{,j} dV \qquad (18)$$

Assume that there exists a strain energy function, W, defined as follows

$$W = \int_0^{\varepsilon_{ij}} \sigma_{ij} d\varepsilon'_{ij} \qquad (19)$$

Thus,

$$W_{,k} = \sigma_{ij} \varepsilon_{ij,k} \qquad (20)$$

which gives

$$I_k = -\int W_{,k} dV + \int (\sigma_{ij} u_{i,k})_{,j} dV = \oint W \nu_k dS + \oint \sigma_{ij} u_{i,k} \nu_j dS \qquad (21)$$

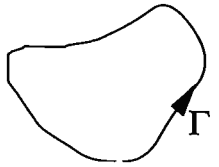

Fig. 6. A loop Γ encompassing a regular region

where the last integral is taken over the path Γ. According to (2)

$$I_k = 0 \qquad (22)$$

which gives

$$\oint (W \nu_k - \sigma_{ij} u_{i,k} \nu_j) dS = 0 \qquad (23)$$

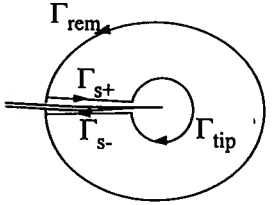

Fig. 7 A regular region in the neighborhood of a crack, encompassed by the path Γ_{tip}, Γ_{s-}, Γ_{rem} and Γ_{s+}.

Here a path independent and vanishing integral is obtained. The integral is path independent under the condition that the material contained by the contour Γ is elastic and regular. The contour in Fig. 6 may be reshaped to the contour in Fig. 7 without violating these conditions. Integration along the crack surfaces (parts Γ_{s+} and Γ_{s-}) does not contribute to the integral. Thus,

$$I_k(\Gamma_{rem}) = -I_k(\Gamma_{tip}) = I_k(-\Gamma_{tip}) \qquad (24)$$

By changing the integration direction for contour Γ_{tip}, as is done after the last equality in (24), it becomes obvious that any integral taken along a contour from the lower crack surface to the upper crack surface anti clock-wise around the crack-tip, give the same value. The J integral is defined by specializing to k = 1

$$J(\Gamma) = \int_\Gamma W dx_2 - \int_\Gamma \sigma_{ij} \nu_j u_{i,1} dS \quad , \qquad (25)$$

where Γ is a path from the lower crack surface to the upper crack surface, e.g., Γ_{rem} or $-\Gamma_{tip}$ in Fig. 7 (cf. Rice [5]). By shrinking the contour into the vicinity of the crack-tip an approximate steady state is obtained

$$\frac{\partial u_i}{\partial a} = -\frac{\partial u_i}{\partial x_1} \qquad (26)$$

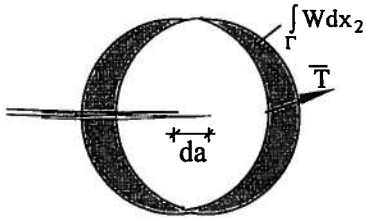

Fig. 8 Steady-state in the near-tip region

The first integral in (25) $\int W dx_2$ then represents the material bound strain energy passing over a contour Γ, assumed to be fixed relative to an advancing crack-tip. The second integral in (25) $\int \sigma_{ij} v_j u_{i,1} dS = \int T_i (\partial u_i / \partial a)\, dS$ (cf. (1) and (26)), represents the work done by tractions T_i acting on the contour during a unit length of crack growth (see Fig. 8). Since the integration path Γ may be shrunk onto the crack-tip J represents the work release rate at the crack-tip.

Example: Consider a substrate with an applied thin film according to Fig. 9. The film is subjected to appreciable residual stress. We wish to calculate the stress intensity factor for a crack growing parallel with and below the interface at a distance that is small compared to the film thickness, h, from the surface of the structure. The analysis can be made for a crack at an arbitrary distance from the free surface in or below the film without difficulties but the calculations will be somewhat lengthier.

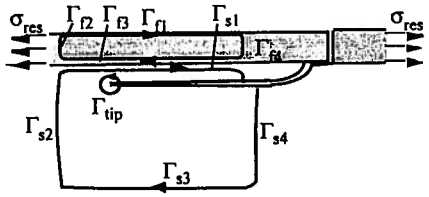

Fig. 9 Integration paths near a steady state crack, growing below a bimaterial surface

Due to path independence $J(\Gamma_{tip}) = J(\Gamma_s) = J(\Gamma_{s1}+\Gamma_{s2}+\Gamma_{s3}+\Gamma_{s4})$. The integral $J(\Gamma_f) = J(\Gamma_{f1}+\Gamma_{f2}+\Gamma_{f3}+\Gamma_{f4}) = 0$, while it is defined for a closed path in the film. Tractions, $T_i = \sigma_{ij} v_j$ and displacement derivatives $u_{i,1}$ are continuos across the bimaterial interface. It is assumed that there is very little in-plane residual stress in the flaking film and part of substrate far behind the crack-tip. The out-of-plane stress remain due to assumed plane strain conditions. By making the contours for $J(\Gamma_s)$ and $J(\Gamma_f)$ very large, only $J(\Gamma_{s1})$, $J(\Gamma_{f2})$ and $J(\Gamma_{f3})$ become non-zero.

$$J(\Gamma_f) = J(\Gamma_{f2}) + J(\Gamma_{f3}) = \int_0^h (1-\nu)^2 \sigma_{res}^2 / E \, dx_2 + \int_{\Gamma_{f3}} T_i \partial u_i / \partial x_1 dx_1 \qquad (27)$$

$$J(\Gamma_s) = -\int_{\Gamma_{s1}} T_i \partial u_i / \partial x_1 dx_1 \qquad (28)$$

$$J(\Gamma_f) = 0 \;\Rightarrow\; J(\Gamma_s) = \tfrac{1}{2}\sigma_{res}\varepsilon_{res} h = \tfrac{1}{2}(1-\nu)\sigma_{res}^2 h / E \qquad (29)$$

If the crack is assumed to follow a pure mode I path one obtains

$$J(\Gamma_s) = J(\Gamma_{tip}) = (1-\nu^2)K_I^2 / E \;\Rightarrow\; K_I = \sigma_{res}\sqrt{\frac{h}{2(1+\nu)}} \qquad (30)$$

6 Cracks Perpendicular to a Bimaterial Interface

It can be shown that only two material parameters need to be considered for plane bimaterial problems. One choice is Dunders' parameters [6] defined as follows

$$\alpha = \frac{G_1(\kappa_2+1) - G_2(\kappa_1+1)}{G_1(\kappa_2+1) + G_2(\kappa_1+1)} \qquad (31)$$

$$\beta = \frac{G_1(\kappa_2-1) - G_2(\kappa_1-1)}{G_1(\kappa_2+1) + G_2(\kappa_1+1)} \qquad (32)$$

where $\kappa_i = 3 - 4\nu_i$ for plane strain and $\kappa_i = (3 - \nu_i)/(1 + \nu_i)$ for plane stress

6.1 Stationary elastic crack

The solution for a crack with its crack plane perpendicular to and the tip at the interface (see Fig. 10) was given by Zak and Williams [7]:

$$\sigma_{ij} = q\,\sigma_o \left(\frac{r\sigma_o^2}{K_{Ic}^2}\right)^{-\lambda} g_{ij}(\theta) \qquad (33)$$

where λ is determined from the generic equation

$$\sin(\pi\lambda)\{\cos(\pi\lambda)-\frac{2(\alpha-\beta)}{1-\beta}(1-\lambda)^2+\frac{\alpha-\beta^2}{1-\beta^2}\}=0 \qquad (34)$$

The distance r from the crack-tip is made non-dimensional by using the material parameters, K_{Ic} and the yield stress, σ_o, q is a load parameter and g_{ij} are known angular functions. Figure 11 shows λ versus α for a few different β. One may note for $\alpha > 0$ that there is very little influence of β on λ.

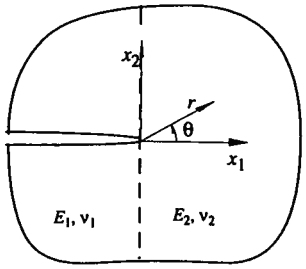

Fig. 10 Crack terminating perpendicular to a bimaterial interface

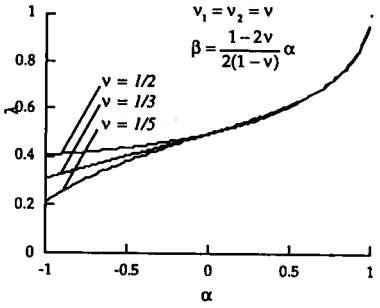

Fig. 11 The exponent λ as a function of the mismatch parameter α

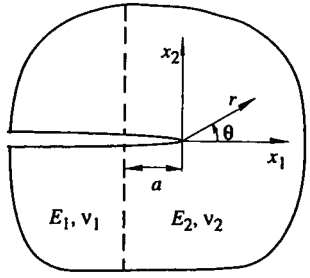

Fig. 12 A crack growing from a bimaterial interface

6.2 Growing elastic crack

Elastic fracture mechanics fail to explain how a crack can penetrate a bimaterial interface from a weaker to a stiffer material. Infinite critical loads are predicted which of course is contradicted by reality. To understand this, a case where the crack has grown a distance a from the interface (see Fig. 12) is considered. The crack-tip is, immediately after it has left the interface, embedded in a homogeneous material. Thus, close to the crack-tip a square-root

singular stress field is developed. The remote field (33), governed by the load parameter q, is supposed not to be effected by the disturbance introduced by a short extension of the crack. Linear elasticity implies a linear relation between remote stresses and near tip stresses. Thus, for dimensional reasons q and K_I must be related according to

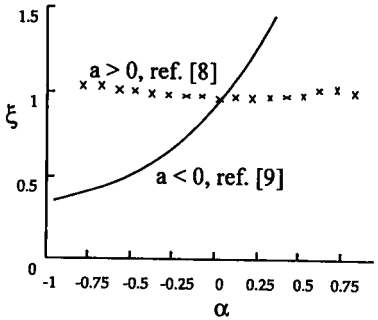

Fig. 13 The K_I scaling parameter ξ as a function of α for $\beta = \alpha/4$.

$$K_I = \xi\, q\sigma_o(2\pi a)^{1/2}\left(\frac{a\sigma_o^2}{K_{Ic}^2}\right)^{-\lambda} = \xi\, qK_{Ic}(2\pi)^{1/2}\left(\frac{a\sigma_o^2}{K_{Ic}^2}\right)^{-\lambda+1/2}, \qquad (35)$$

where $\xi = \xi(\alpha, \beta)$ is an undetermined non-dimensional constant of proportionality, depending on the material mismatch properties only. Thus, (35) describes the load transfer to the tip for different elastic mismatches. In Fig. 13 the α-dependence of ξ obtained from a finite element analysis [8] is shown. Schmauder and Müller [9] analyzed a crack approaching an interface ($a < 0$) using Erdogan's integral equation technique. Their results are included in Fig. 13. The behavior for $a > 0$ as compared with that for $a < 0$ is surprisingly different.

For plastic yielding at a small scale compared with the crack advance a, it may be assumed that crack growth occurs when $K_I = K_{Ic}$, i.e. $q_c = (1/\xi\sqrt{2\pi})(a\sigma_o^2/K_{Ic}^2)^{\lambda-1/2}$. Equation (35) explicitly shows that as the crack approach an interface to a weaker material, i.e., if $\lambda > 1/2$, q_c vanishes and q_c becomes unbounded as the crack approach an interface to a stiffer material, i.e., for $\lambda < 1/2$. This is sketched in Fig. 14 where the critical load, q_c, is plotted versus the position, a, of the crack-tip.

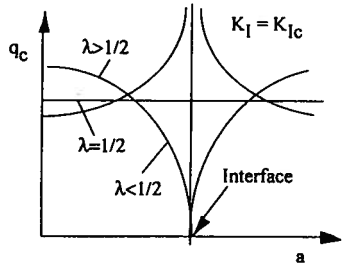

Fig. 14 Critical load q_c as a function of the crack length a

The result is found under two assumptions, 1) that the K_I-controlled autonomy prevails and 2) that the crack follows a straight and

perpendicular path to the interface. In fact as a crack approach an interface to a stiffer material for which $\lambda < 1/2$, either of two things may happen: 1) The non-linear region at the crack-tip may become of the size of the distance left to the interface. Thus, the K_I controlled autonomy is no longer guaranteed. The result can be that the crack grows across the interface under the control of another load parameter than K_I. This is explained in section 6.3 and 6.4. 2) The crack may become path unstable. Thus, a slight deviation from the straight path causes a redistribution of the near-tip stress state that promotes an increased deviation. examples of this is examined in section 9.

6.3 Stationary elastic-plastic crack

Assume that a crack is terming perpendicularly at a bimaterial interface where one or both materials are elastic-plastic. The film contains a crack and has the yield stress τ_o. The substrate has the yield stress $\gamma\tau_o$. Stress distributions for a broad range of elastic moduli and yield strength mismatches may be constructed using slip-line solutions [10, 11]. Fig. 15 shows the slip-line solutions for two different mismatches in yield stress.

The resulting stresses can be used to understand the effect of mechanical properties mismatch on the competition between crack deflection into the interface and crack penetration into the base material. Small defects, with depths smaller than the film thickness, distributed at the surface of the substrate, are subjected to stresses that may be computed from the slip-line fields. A yielded film such as the one in Fig. 15b induces a high stress (about $5\tau_o$) parallel with the interface on the substrate side [10]. Driven by the stress the small defects may grow and ultimately the substrate fractures. A detailed discussion of this can be found in [10].

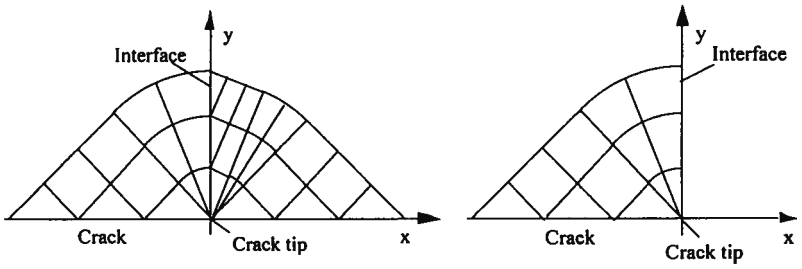

Fig. 15 Near-tip slip line fields in film and substrate. a) $\gamma > 1$; b) $\gamma \to \infty$

6.4 Growing elastic-plastic crack

To treat the elastic plastic generalization of the problem defined in Fig. 12 one have to focus on the stress and strain field that develops inside the plastic region. Delfin et al. [8] observed that the crack opening displacement at the initial stage of crack growth is reversed as compared to what would be expected from a K_I-based prediction (cf. Fig. 17). Thus, a crack growing from an interface into a weaker material at a constant remote load will experience an increasing load at the crack-tip. This crack is likely to be unstable as it is growing. The opposite happens as a crack grows into a stiffer material. Here one would expect the crack to be unstable if K_I-control would be at hand, while a constant remote load lead to increasing K_I in the elastic case. However, calculations of the near-tip plastic field show that the crack-tip opening displacement is decreasing suggesting that there, quite opposed to expectations for an elastic case, will be an initial phase of stable crack growth.

The asymptotic near-tip field for a crack growing in a homogeneous elastic perfectly-plastic solid under small scale yielding conditions has been derived by Rice and Sorensen [12] and Drugan, et al. [13]. The separation of the crack surfaces, close to the crack-tip, is of the form

$$\delta = \frac{A}{\sigma_o}\frac{dJ}{da} r + B\frac{\sigma_o}{E_2} r \ln\left[\frac{eR}{r}\right], \tag{36}$$

where J is the J-integral, e is the natural logarithm base,

$$R = \frac{E_2 J}{\sigma_o^2} s \quad \text{and} \quad J = \frac{(1-\nu_2^2)}{E_2} K_I^2 \tag{37}$$

where σ_o is the yield stress in the initially uncracked material. The parameters A, B and s have been numerically estimated by several investigators. A suitable choice could be A, B and s, equal to 0.6, 5.3 and 0.27 respectively.

Fig. 17 a and b is showing the crack opening displacements and height of plastic zone versus extent of crack growth for α = -0.8, -0.4, 0, 0.4 and 0.8 at a small distance from the crack-tip[8]. The results provide a possibility to predict the toughness of materials subjected to fracture induced by a cracked film.

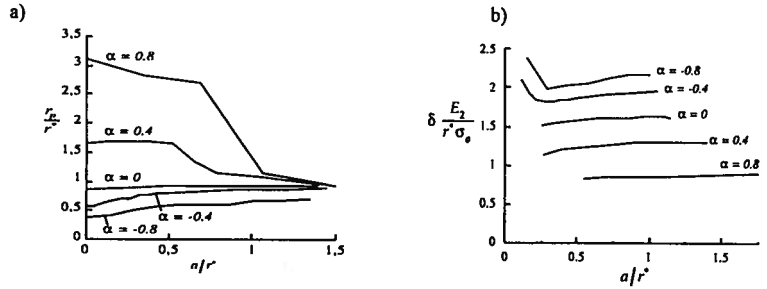

Fig. 16 a) Height of the plastic zone over the crack plane; b) Crack-tip opening displacements. The displacements δ are measured at 0.05r*. The scaling length parameter $r^* = (K_{Ic}/\sigma_o)^2$

7 Crack in the Interface Between two Dissimilar Materials

The solution for a crack situated in the plane between two dissimilar materials is given by (33). However, here λ is given by (cf. Shih [14])

$$\lambda = \frac{1}{2} - i\varepsilon \qquad (38)$$

where

$$\varepsilon = \frac{1}{2\pi} \ln\left(\frac{1-\beta}{1+\beta}\right) \qquad (39)$$

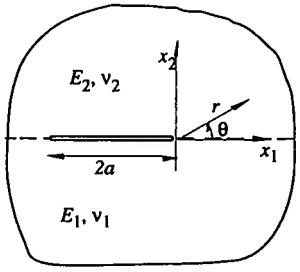

Fig. 17. A crack in a bimaterial interface

The material parameter ε is for realistic material combinations very small and usually below 0.1, e.g., for SiO_2 on Al_2O_3 ε = 0.075. The stress ahead of the crack-tip (θ = 0) becomes

$$\sigma_{22} + i\sigma_{12} = \frac{1}{2}\left(\sigma_{22}^{\infty} + i\sigma_{12}^{\infty}\right)(1+i\varepsilon)(L/r)^{1/2-i\varepsilon} \qquad (40)$$

where σ_{22}^{∞} and σ_{12}^{∞} are stresses at a large distance from the crack. Because of the oscillating nature of the stresses one may compute the distance to the position where the normal stress, σ_{22}, first vanish as the crack-tip is approached. By using the fact that ε is small one obtains a simplified expression from (40). For SiO_2 on Al_2O_3

$$r = \mathrm{Lexp}\left[-\frac{\pi}{2\varepsilon}\arctan(\sigma_{22}^{\infty}/\sigma_{12}^{\infty})\right] = \begin{cases} 8\times10^{-10}\,\mathrm{L} & \text{for} \quad \sigma_{12}^{\infty} = 0 \\ 3\times10^{-5}\,\mathrm{L} & \text{for} \quad \sigma_{12}^{\infty} = \sigma_{22}^{\infty} \end{cases}, \qquad (41)$$

which in practice hardly can be observed in either of the two load cases. It is important to realize that fracture process regions generally are very small, especially at brittle fracture but the small distances found in (41) is even so likely to be within the fracture process regions. Therefor the conditions in the fracture process region are expected to be effected by the oscillatory character of the near-tip field. A strong dependence on fracture toughness of mode mixity $\sigma_{12}^{\infty}/\sigma_{22}^{\infty}$ has been observed in experiments [15]. Micro mechanical studies of mixed mode fracture of interfaces have been performed by Sun et al. [16] and Wang and Ståhle [17].

8 Crack Path Stability

A commonly made assumption in crack growth analysis is that the crack remain in its original plane. In this section the path of an edge crack in a compliant elastic layer is considered. The plane of the initially straight crack form an angle, θ_o, to the free surface of the layer. The load is a force couple applied to open the crack mouth parallel to the interface as shown in Fig. 18. The growing crack is assumed to follow a path along which the mode II stress intensity factor vanishes. In [18] cracks in an elastic layer on two different substrates was studied. The boundary element method (BEM) was used for calculation of growing cracks. Figs. 19 a and b show the resulting crack paths for a rigid and an inextendable flexible substrate respectively. With inextendable flexible is meant that displacement parallel with the edge bonded to the substrate and tractions normal to the edge vanish.

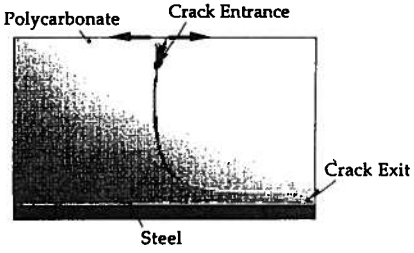

Fig. 18. An model experiment showing path unstable crack growth.

The crack path leading straight and perpendicular to the bimaterial interface is unstable for rigid substrates. For an inextendable flexible substrate an unstable path parallel with the sides of an infinite layer is identified. Cracks with a small inclination to the surface return to this surface irrespective of the boundary conditions at the bimaterial interface. Cracks with a large inclination also return to the surface for rigid substrates but approach the bimaterial interface for inextendable flexible substrate. The results are compared with experimental results and discussed in view of a characterization of stable crack paths in [18].

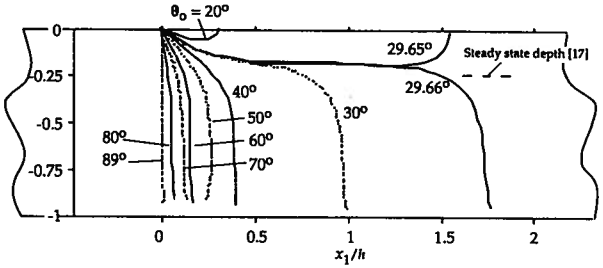

Fig. 19 a. Crack paths in a film on a rigid substrate. θ_o is the angle between the initial crack and the traction free surface

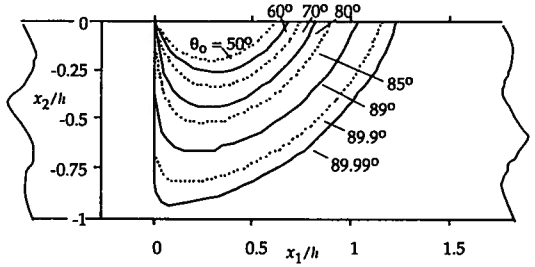

Fig. 19 b. Same as Fig. 19a for a rigid substrate.

9 Cracks Parallel with a Bimaterial Interfaces

A frequent observation is that a crack deflects following a curved path as described in the previous section. After a short distance the crack may run almost parallel with the interface. A steady state path for which $K_{II}/K_I = 0$ can often be found. BEM and FEM are excellent tools for examination of cracks growing along steady state paths. However here a simple beam model is described. This model give fairly accurate results and requires much less effort.

9.1 Simplified analysis of steady-state crack depth

A crack may either find a steady-state path parallel to the interface, approach the interface or return to the free surface. Wavy crack paths that exceptionally have been observed are not considered here. In the case when the crack return to the surface a fragment is formed. Fig. 4 shows the geometry for the simplified calculations. The expression giving M_2 is somewhat lengthy but is easily calculated from simple beam theory.

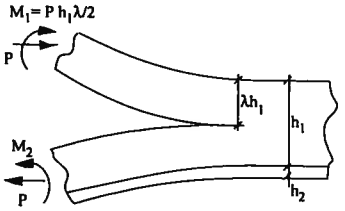

Fig. 20 Geometry for the simplified calculations for steady-state cracks.

A symmetry for stresses at the base of the beams A and B is sought by a variation of the distance λh_1, between the stress free surface of the layer and the crack plane [14]. Symmetry paths ($K_{II}/K_I=0$) can either be stable with $d(K_{II}/K_I)/d\lambda <0$ or unstable with $d(K_{II}/K_I)/d\lambda >0$. Fig. 21 shows a map of possible paths for different combinations of λ and h_1/h_2.

For thin beams $h_1/h_2 > 13.6$ an unstable path was found at $\lambda = \lambda_2$. This means that any straight crack at $\lambda < \lambda_2$ would form a kink in a direction towards the surface of the layer ($\lambda =0$). Reversed at $\lambda > \lambda_2$ a kink would be formed in a direction towards the interface ($\lambda = 1$).

For the interval $6.9 < h_1/h_2 < 13.6$ a stable path is found at $\lambda = \lambda_1$ and an unstable path at $\lambda = \lambda_2 < \lambda_1$. This means that a straight crack at $\lambda < \lambda_2$ would approach the layer surface ($\lambda = 0$), a straight crack in $1 > \lambda > \lambda_2$ would approach the steady-state path at $\lambda = \lambda_2$.

In the region $h_1/h_2 < 6.9$ any straight path in the layer would result in a kink directed towards the stress free surface of the layer. This suggests that all cracks will deflect and turn towards the layer surface ($\lambda = 0$). Other loads can be studied with the same method. These paths are of interest since the

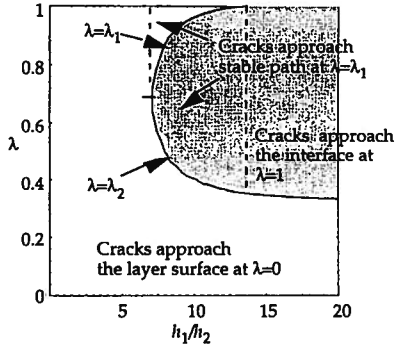

Fig. 21 Stable and unstable paths for steady-state cracks for different height ratios h_1/h_2, [19].

resistance to delamination does not involve the strength of the interface whereas the crack grow in a homogeneous material, i.e. either the film or the substrate.

References

[1] M. L. Williams, Journal of Applied Mechanics 24, pp. 109-114 (1957)

[2] G. I. Barenblatt, Advances in Applied Mechanics 7, pp. 55-129 (1962)

[3] K. B. Broberg, Journal of the Mechanics and Physics of Solids 23, pp. 215-237 (1975)

[4] W. F. Brown and J. E. Shrawley, Plane Strain Crack Toughness Testing of High Strength Metallic Materials ASTM Special Technical Publication 410 (1966)

[5] J., R. Rice, Fracture II, Academic Press, New York, pp. 191-311 (1968)

[6] J. Dunders, Edge-bonded dissimilar Orthogonal Elastic Wedges, Journal of Applied Mechanics 36, pp. 650-652 (1969)

[7] A. R. Zak and M. L. Williams, Crack Point Singularities at a Bi-material Interface, Journal of Applied Mechanics 30, pp. 142-143 (1963)

[8] P. Delfin, J. Gunnars and P. Ståhle, Fatigue and Fracture of Engineering Materials and Structures 18, no. 10, pp. 1201-1212 (1995)

[9] S. Schmauder and W. H. Müller, International Journal of Fracture 51, R21-R27 (1991)

[10] P. Ståhle and C. F. Shih, Cracking in thin films and substrates, Material Research Society Symposium Proceedings 239, Boston, pp. 567-572 (1992)

[11] M. Y. He, T. Z. Ning and R. M. McMeeking, Cracking in thin films and substrates, Material Research Society Symposium Proceedings 239, Boston, pp. 572-577 (1992)

[12] J. R. Rice and E. P. Sorensen, Journal of the Mechanics and Physics of Solids 26, pp. 163-186 (1978)

[13] W. J. Drugan, J. R. Rice and T.-L. Sham, Journal of the Mechanics and Physics of Solids 30, pp. 447-473 (1982)

[14] C. F. Shih, Materials Science and Engineering, A170 (1991)

[15] K. M. Liechti and Y.-S. Chai, Journal of Applied Mechanics, in Press (1992)

[16] Y. M. Sun, G. E. Beltz and J. R. Rice, Materials Science and Engineering, A130 (1993)

[17] T. C. Wang and P. Ståhle, A dislocation Model for Bimaterial Interface Failure,. Submitted (1997)

[18] J. Gunnars, P. Ståhle and T. C. Wang, Computational Mechanics, Vol. 9, pp. 545-552 (1997)

[19] P. Ståhle, J. Gunnars and P. Delfin, Acta Mechanica Solida Sinica, Vol. 8, S. Issue, pp. 579-583 (1995)